ISET Journal of Earthquake Technology, Paper No. 506, Vol. 46, No. 3-4, Sept.-Dec. 2009, pp. 125–132

SIMULATION OF STRONG GROUND MOTIONS OF WENCHUAN EARTHQUAKE BY STOCHASTIC FINITE-FAULT METHOD

Guoxin Wang and Jiaping Shi

State Key Laboratory of Coastal and Offshore Engineering
Dalian University of Technology, Dalian 116024, China

ABSTRACT

The 2008 Wenchuan earthquake (M_s = 8; May 12, 2008; Sichuan, China) had caused a great loss to both life and property. We compute the accelerograms of Wenchuan strong motions by the stochastic finite-fault method and obtain the isolines of peak ground acceleration. This study provides a reasonable interpretation of the causes and degree of the structural destruction caused by the strong ground motions during this event. This also improves the stochastic finite-fault method by incorporating the structural aseismic capability.

KEYWORDS: Wenchuan, Stochastic Finite-Fault Method, Near-Fault Strong Ground Motion

INTRODUCTION ABOUT WENCHUAN EARTHQUAKE

The 2008 Wenchuan earthquake had a magnitude of $M_s 8$ or $M_w 7.9$ according to the China Earthquake Administration (CEA). The epicenter was in the Wenchuan county (31.0ºN, 103.4ºE), 80 km west-northwest of the provincial capital city of Chengdu, with its main tremor occurring at 14:28:01.42 CST (or, 06:28:01.42 UTC) on May 12, 2008. This earthquake was felt as far as Beijing (1,500 km away) and Shanghai (1,700 km away), where office buildings swayed with the tremor. The earthquake was also felt strongly in the nearby counties, with the highest MMI (= XI) observed in Beichuan. It is considered as the deadliest and strongest earthquake to hit China since the 1976 Tangshan earthquake.

This earthquake occurred along the long and complex Longmenshan fault consisting of three parallel faults and several transversal faults (see Figure 1), caused due to the thrusting along the border of the Indo-Australian and Eurasian plates. The rupture initiated at the middle of the fault known as Yingxiu-Beichuan fracture and lasted close to 120 s, with major energy released during the first 80 s. Starting from Wenchuan, the rupture propagated at an average speed of 3.1 km/s in the north-east direction, thus rupturing a total length of about 300 km. The maximum displacement of the fault was 9 m. The relative motion between the India and Eurasian plates causes large-scale structural deformations inside the Asian continent, thus resulting in the crustal thinning of the Qinghai-Tibet Plateau, uplift of its landscape, and an eastward extrude. Near the Sichuan basin, the east-northward movement of the Qinghai-Tibet plateau meets with a strong resistance from the South China block, thus causing a high degree of stress accumulation in the Longmenshan thrust formation. This finally caused a sudden dislocation in the Yingxiu-Beichuan fracture, thus leading to the violent earthquake of $M_s 8$ (CEA[1]).

The purpose of this paper is to estimate the strong ground motion distribution, which will be helpful in understanding and analyzing the reason and degree of structural destruction due to this event.

STOCHASTIC FINITE-FAULT SIMULATION METHOD—MOMENT ROTATION RELATION

1. Source Parameters

1.1 Source Spectral Model

The source spectral model $S(M_0, f)$ is expressed as follows (Wang, 2001), which is a modification to the traditional ω^2 model by linking the coefficients a and b with magnitude in order to reduce the

obvious "sag" phenomenon in the transitional frequency range between the low and high frequencies as magnitude increases:

$$S(M_0, f) = \frac{M_0}{\left[1+(f/f_0)^a\right]^b} \tag{2.1}$$

where M_0 is seismic moment, f represents frequency, f_0 is corner frequency, and the coefficients a and b are 3.5–0.3M and 2/a, respectively. These are estimated from the strong ground motion recordings.

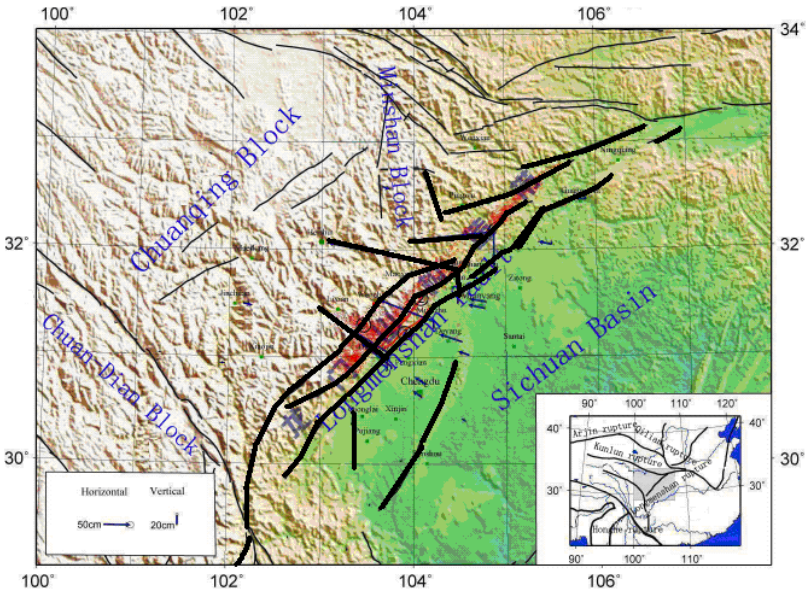

Fig. 1 Longmenshan fault (from the website of CEA)

1.2 Main Source Size

Kanamori and Anderson (1975) suggested a theoretical relation between the rupture area S, stress drop $\Delta\sigma$, and seismic moment M_0 of an earthquake based on the seismological theory,

$$\log M_0 = 1.5\log S + \log \Delta\sigma + \log C \tag{2.2}$$

where M_0 can be computed from the moment magnitude M_W, and C is the constant related to the fault type as suggested by Hanks and Kanamori (1979):

$$\log M_0 = 1.5M_W + 16.1 \tag{2.3}$$

According to the definition of M_0, it is known that

$$M_0 = \mu SD \tag{2.4}$$

The value of $\Delta\sigma$ could be expressed as

$$\Delta\sigma = C'u\frac{\bar{D}}{\tilde{L}} \tag{2.5}$$

where $\bar{D}$ is the mean slip on the fault, and shear modulus u is equal to 3.1×10^{11}. The factor C' is related with the fault length $\tilde{L}$ as

$$\text{disk rupture:} \quad C' = \frac{7\pi}{16},\ \tilde{L} = r$$

$$\text{thrust fault:} \quad C' = \frac{16}{3\pi},\ \tilde{L} = W \tag{2.6}$$

$$\text{strike-slip fault: } C' = \frac{2}{\pi},\ \tilde{L} = W$$

$$\text{down dip-slip fault: } C' = \frac{4(\lambda+\mu)}{\pi(\lambda+2\mu)},\ \tilde{L} = W$$

r is the disk radius, W the fault width, and λ the Lamé constant. $\tilde{L}$ could be expressed as

$$\log \tilde{L} = 0.5M_W + 5.4 + \frac{2}{3}\log C + \log C' - \frac{1}{3}\log \Delta\sigma \tag{2.7}$$

The parameter C in Equation (2.2) can be expressed as

$$\text{disk rupture:} \quad C = \frac{16}{7\pi^{3/2}} = 0.4105$$

$$\text{thrust fault: } C = \frac{3\pi}{16} = 0.589 \tag{2.8}$$

$$\text{strike-slip fault: } C = \frac{\pi}{2}\left(\frac{W}{L}\right)^{1/2}$$

$$\text{down dip-slip fault: } C = \frac{\pi(\lambda+2\mu)}{4(\lambda+\mu)}\left(\frac{W}{L}\right)^{1/2}$$

These theoretical equations can be used to calculate rupture radius for the disk fault model or rupture width for the rectangle fault model. For a rectangle fault model, the rupture area S is equal to LW; hence, by substituting the value of S into Equation (2.4) and combining it with Equations (2.3), (2.5) and (2.7), we obtain

$$\log L = 0.5M_W + 5.3 - \frac{4}{3}\log C - \log C' - \frac{1}{3}\log \Delta\sigma \tag{2.9}$$

On substituting Equations (2.5)–(2.7), the relation between the parameters $\bar{D}$ and M_W can be obtained as follows:

$$\log \bar{D} = 0.5M_W + 5.4 + \frac{2}{3}(\log C + \log \Delta\sigma) - 11.5 \tag{2.10}$$

The details of this derivation are given in Wang (2004) and are therefore not repeated here.

1.3 Subsource Parameters

The preliminary requirement in dividing the main source into various subsources is that the cumulative energy released by the subsources should be equal to that released by the main source. This will ensure that the seismic moment summation from all subsources is equal to the total seismic moment from the main source. Wang (2001) and Wang and Shi (2008) suggested that there exists one suitable subsource size, ΔL, corresponding to the subsource magnitude M_z that could simulate better accelerograms, once the event magnitude M and total rupture length L of the fault are known. Wang (2001, 2008) used the following equation based on the previous research results (Beresnev and Atkinson, 1997; Shi et al., 2005; Tao and Wang, 2003) to compute the source size:

$$\log \Delta L = \log L - 0.5(M - M_z) \tag{2.11}$$

The subsource size obtained from the above equation corresponds to the subevent magnitude and could be treated as a point source. Once ΔL is determined, the seismic moment of each subsource could be estimated, and thus, the number N_e of subevents could be obtained from the seismic moment of the main event:

$$\text{Subevent seismic moment: } M_e = \Delta\sigma.A.\Delta L \tag{2.12}$$

$$\text{Number of subevents: } N_e = \frac{M_0}{M_z} \tag{2.13}$$

Hence, the accelerogram $a(t)$ caused by all subevents could be generated by superposing the initial accelerograms with appropriate delays from those subevents:

$$a(t) = \sum_{i=1}^{N_L} \sum_{j=1}^{N_W} a_{ij}\left(t + \Delta t_{ij}\right) \tag{2.14}$$

where N_L and N_W are the numbers of subevents along the fault length and width, respectively, and N_L x $N_W = N_e$; Δt_{ij} represents the time delay of wave propagating from the fixed starting point of the rupture on the fault to the *i-j*th subsource center and then to the expected analyzing site; and $a_{ij}(t)$ is the accelerogram caused by the *i-j*th subsource.

2. Modeling

We model the area bounded by 98ºE and 112ºE, and by 28ºN and 37ºN, around the Longmenshan fault. The fault dimension for the Wenchuan earthquake is about 320×30 km, which could be divided into 48 subsources with the size of 20×10 km in this study according to Equation (2.11). The seismic moment of each subsource therefore can be estimated as (Beresnev and Atkinson, 1997)

$$M_e = \Delta\sigma.S.\Delta L = \Delta\sigma.W.\Delta L^2 = 1.0\times10^{19} \text{ N.m} \tag{2.15}$$

and the number of subevents will be

$$N_i = \frac{M_0}{M_e} = \frac{1.4\times10^{21}}{1.0\times10^{19}} = 140 \tag{2.16}$$

Thus, there are 48 subsources and 140 subevents (that could represent the actual earthquake) that are distributed on the fault plane and indicate that slip distribution may be different in each subsource. Normally, there are more subevents around the hypocenter than the edge of the fault. The distribution of subevents is shown in Figure 2. The actual distribution, however, may be different because of the inversion results. The effect of distribution is not large, as observed from the sensitivity analysis of the source parameter variation. It may be noted that the hypocenter of the Wenchuan earthquake is treated here as the starting point of the fault rupture process.

1	3	4	5	5	4	4	3	3	3	3	2	2	2	1	1
2	3	4	5	★ 5	4	4	3	3	3	3	2	2	2	1	1
2	3	4	5	5	4	4	3	3	3	3	2	2	2	1	1

hypocenter

Fig. 2 Subsource distribution

3. Parameter Estimation

Various seismological parameters of the main source and subsources, including the exact fault length, width, depth, and striking angle, could be estimated by the method introduced above as shown in Table 1. The geological data around the Wenchuan region are also listed in Table 2. The nonlinear attenuation is assumed to be frequency-independent here.

4. Data and Result Analysis

4.1 Data

In order to highlight the differences in theoretical and real situations and to understand the reasons that cause such differences, we simulate accelerograms at two seismological stations, Chengdu (104.06ºE, 30.67ºN) and Lanzhou (103.50ºE, 36.03ºN), where the recorded time histories are available. Figure 3 shows the random accelerograms simulated for these stations. The recorded accelerograms for these

stations are shown in Figure 4. It may be observed that peak ground acceleration (PGA) is about 610 cm/s^2 at the Chengdu station and 80 cm/s^2 at the Lanzhou station.

Table 1: Source Parameters

Event Time	14:28 CST; May 12, 2008
Epicenter	30.94°N, 103.47°E
Hypocenter Depth	14 km
Breaking Mode	Unilateral, toward NE
Fault Type	Dextrorotation Strike Fault
Striking and Dip Angles	N70ºE; 40°
Main Fault Dimensions (length×width)	320×30 km
Subfault Dimensions (length×width)	20×10 km
Subsource Number	48
Subevent Number	140
Fault Length	3–20 km
Main Event Seismic Moment M_0	1.4×10^{21} N.m
Subevent Seismic Moment M_e	1.0×10^{19} N.m
Moment Magnitude M_w	8.3
Mean Slip	1.5 m
Stress Drop	2.5×10^{6} Pa
Shear Velocity β	3.5 km/s
Breaking Velocity v_r	3.0 km/s
Rupture Duration	120 s

Table 2: Geological Parameters

Upper Depth (m)	Thickness (m)	Shear Velocity (m/s)	Density (kg/m^3)	Q
0	100	1500	2200	150
100	1000	2800	2500	200
1100	5000	3200	3000	350
6100	50000	3600	3200	400

It is observed from Figures 3 and 4 that the simulated as well recorded time series are of relatively higher amplitudes and longer duration in the near-fault region. The simulated and recorded accelerograms are comparable both in amplitudes and wave forms showing the acceleration variation process during the earthquake. This indicates that the method and parameters adopted here are suitable for analyzing the strong ground motion variation for such a strong earthquake.

4.2 Result Analysis

To study the spatial variation of PGA in Wenchuan and the surrounding region, we simulated accelerograms at the points of 0.2º×0.2º grid from 98º to 112ºE and from 28º to 37ºN and estimated the PGA isolines (see Figure 5). It is observed that the PGA distribution is not symmetrical about the fault-axes. It is greater than 600 cm/s^2 at some locations, and the mean PGA is about 400 cm/s^2 along the 300-km long fault. Also, the PGA is higher than 300 cm/s^2 within about 100 km perpendicular to the fault, which may cause substantial disaster. Further, the directivity effect in Figure 5 is very typical, especially in the near-fault region: the variation of PGA is significant in the north-east direction and small in the south-west direction, as the fault ruptures from the south-west direction to the north-east direction. All of these preliminary phenomena are reasonably captured by our simple and easy method.

The isolines obtained from the recordings of the Wenchuan earthquake in the east-west direction are shown in Figure 6, while the maximum recorded PGA is 632.9 cm/s^2. It may be observed from the comparison of Figures 5 and 6 that both are basically similar, with similar trends in amplitudes and distribution. Hence, any practical situation may be represented, if the method and parameters are selected properly.

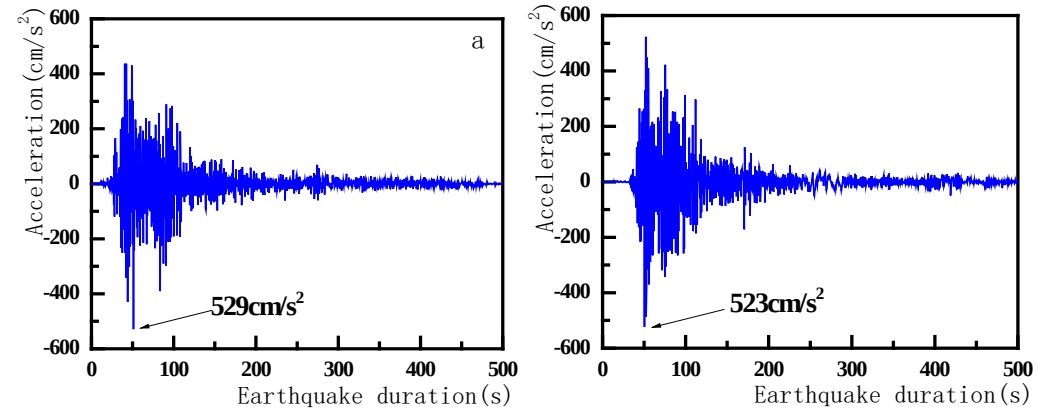

(a)

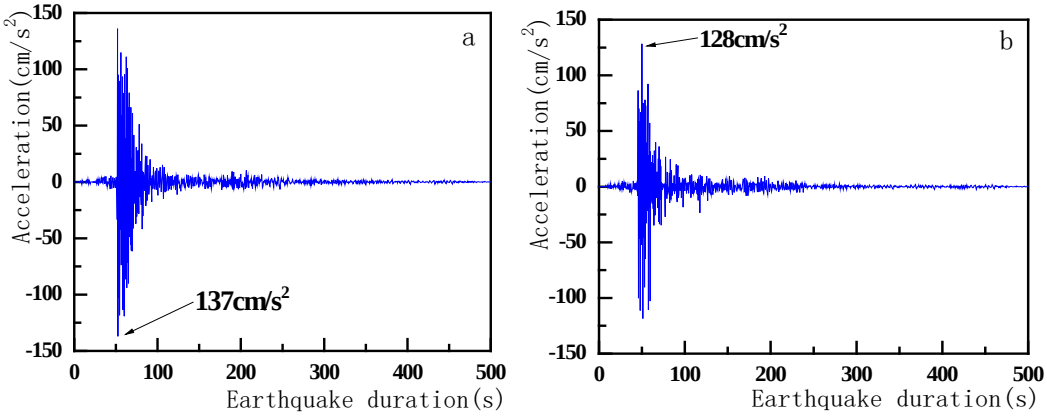

(b)

Fig. 3 Simulated accelerograms at (a) Chengdu and (b) Lanzhou stations

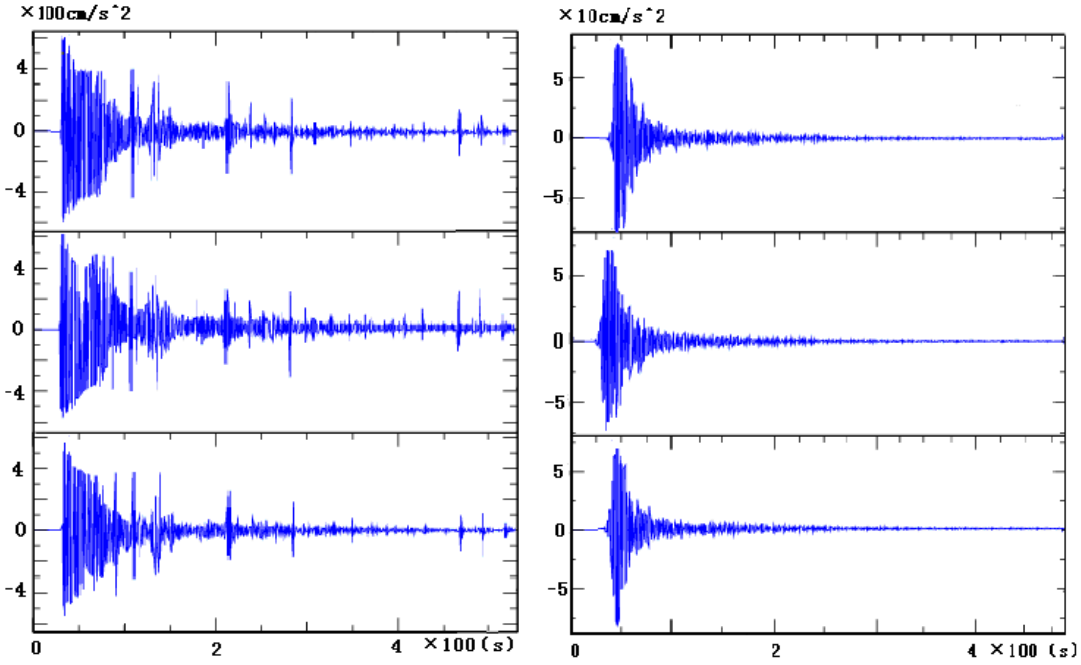

(a) (b)

Fig. 4 Recorded accelerograms at (a) Chengdu station (at the epicentral distance of 64 km) and (b) Lanzhou station (at the epicentral distance of 567 km) (the upper, middle, and bottom frames refer to the two horizontal and one vertical accelerograms, respectively)

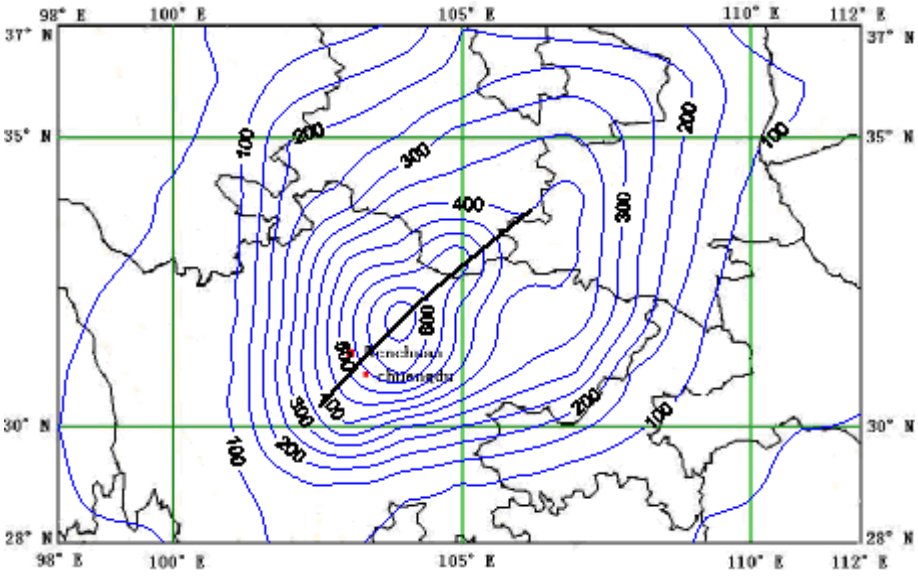

Fig. 5 Estimated PGA isolines of Wenchuan earthquake

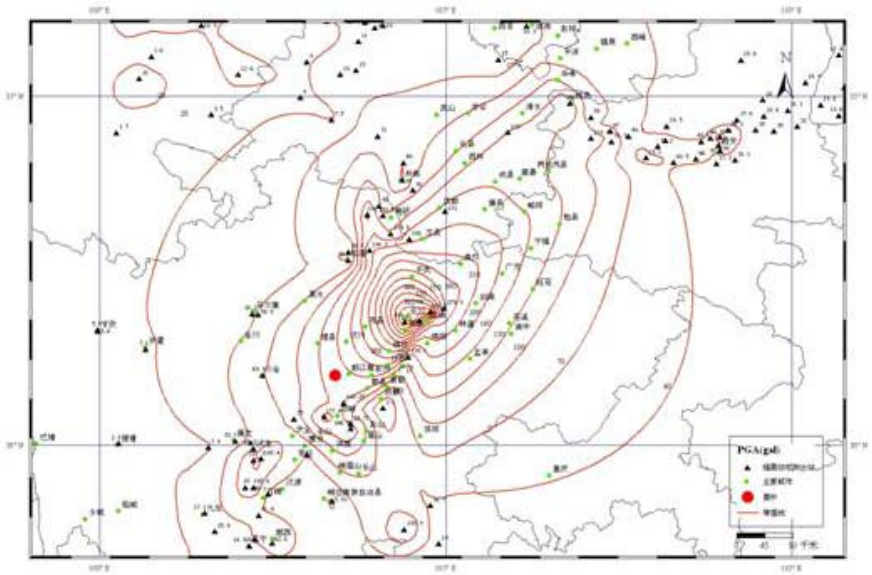

Fig. 6 Recorded PGA isolines of Wenchuan earthquake in east-west direction (China Earthquake Information Network[2])

CONCLUSIONS

Following conclusions can be drawn from the analysis of the results:

1. The Wenchuan earthquake is characterized by a large affected region, huge energy release, longer fault size, larger PGAs, and longer durations. All of these characteristics could be simulated reasonably well by our method.
2. The highest PGA is not in the epicenter area (at Wenchuan) but at Beichuan in the Mao county. The directivity effect has been found to be dominant during this earthquake and this has caused huge casualties and economic losses in the region.
3. The PGA distribution is not symmetrical around the fault; this indicates the complexity of the wave propagation and of the local-site effects on ground motions.
4. The PGA isolines from the simulated accelerograms and recordings indicate that theoretical methods can approximately lead to true PGA distributions between these isolines, provided the methods and parameters are chosen properly. The stochastic finite fault method is one of such simple and easy tools.

Several problems that still need to be addressed in future works to accurately predict the expected ground motions are as follows:

1. It is known that an earthquake source may not be treated as a "point" source when the earthquake magnitude is large, as in the case of the Wenchuan earthquake. Hence, although a relatively small magnitude has been adopted for each subsource, in simulating accelerograms in the proposed finite-fault method, for consistency with the point source model, some other related aspects still need to be improved to make the simulated results match with the recorded data, especially for large magnitudes and for the middle- to far-distance range.
2. Uncertainties in the physical parameters adopted in analyzing a process, e.g., stress drop, have obvious effects on the results. Hence, how to reduce these effects is our main target for the future studies.
3. The assumption of uniform geological distribution for a large region may not be suitable in modeling the wave propagation, as we have done in our analysis. Thus, the simulated results may sometimes differ from the recorded ones.

REFERENCES

1. Beresnev, I.A. and Atkinson, G.M. (1997). "Modeling Finite-Fault Radiation from the ω^n Spectrum", Bulletin of the Seismological Society of America, Vol. 87, No. 1, pp. 67–84.
2. Hanks, T.C. and Kanamori, H. (1979). "A Moment Magnitude Scale", Journal of Geophysical Research, Vol. 84, No. B5, pp. 2348–2350.
3. Kanamori, H. and Anderson, D.L. (1975). "Theoretical Basis of Some Empirical Relations in Seismology", Bulletin of the Seismological Society of America, Vol. 65, No. 5, pp. 1073–1095.
4. Shi, Y., Chen, H., Li, M. and Lu, Y. (2005). "The Study and Application of Stochastic Finite Faults Method in Ground Motion Synthesizing", Earthquake Engineering and Engineering Vibration, Vol. 25, No. 4, pp. 18–23 (in Chinese).
5. Tao, X.-X. and Wang, G.-X. (2003). "Rupture Directivity and Hanging Wall Effect in Near Field Strong Ground Motion Simulation", Acta Seismologica Sinica, Vol. 16, No. 2, pp. 205–212.
6. Wang, G.-X. (2001). "Study on Strong Ground Motions", Ph.D. Thesis, Institute of Engineering Mechanics, Harbin, China (in Chinese).
7. Wang, H. (2004). "Finite-Fault Model for Predicting Near-Site Ground Motion", Ph.D. Thesis, Institute of Engineering Mechanics, Harbin, China (in Chinese).
8. Wang, G.-X. and Shi, J.-P. (2008). "Study and Simulation on Near-Site Strong Ground Motions", Seismological Research of Northeast China, Vol. 24, No. 2, pp. 4–10.

[1] Website of CEA, www.cea.gov.cn/manage/html/8a8587881632fa5c0116674a018300cf/_content/08_05/30/1212119940937.html

[2] Website of China Earthquake Information Network, www.csi.ac.cn/manage/html/4028861611c5c2ba0111c5c558b00001/_content/08_06/06/1212732534049.html